Atmospheric Environment 94 (2014) 274–286

Contents lists available at ScienceDirect

Atmospheric Environment

journal homepage: www.elsevier.com/locate/atmosenv

An integrated $PM_{2.5}$ source apportionment study: Positive Matrix Factorisation vs. the chemical transport model CAMx

M.C. Bove [a], P. Brotto [a], F. Cassola [a], E. Cuccia [a], D. Massabò [a], A. Mazzino [a], A. Piazzalunga [b], P. Prati [a,*]

[a] Dept. of Physics & INFN, University of Genoa, via Dodecaneso 33, 16146 Genoa, Italy
[b] Dept. of Environmental and Territorial Sciences, Università degli Studi di Milano-Bicocca, Piazza della Scienza 1, 20122 Milan, Italy

HIGHLIGHTS

- Receptor (PMF) and Chemical Transport (CAMx) Models were used in the same study area.
- Major $PM_{2.5}$ emission sources were singled out using both the approaches.
- A critical revision of PMF profiles provided the apportionment of secondary aerosol.
- Criteria for classification of $PM_{2.5}$ sources with both the approaches were harmonised.
- Source apportionment by PMF and CAMx turned out to be in fair agreement.

ARTICLE INFO

Article history:
Received 27 September 2013
Received in revised form
16 April 2014
Accepted 13 May 2014
Available online 14 May 2014

Keywords:
$PM_{2.5}$
Source apportionment
Receptor models
Chemical transport models

ABSTRACT

Receptor and Chemical Transport Models are commonly used tools in source apportionment studies, even if different expertise is required. We describe an experiment using both approaches to apportion the $PM_{2.5}$ (i.e., particulate matter with aerodynamic diameters below 2.5 μm) sources in the city of Genoa (Italy). A sampling campaign was carried out to collect $PM_{2.5}$ samples daily for approximately six month during 2011 in three sites. The subsequent compositional analyses included the speciation of elements, major ions and both organic and elemental carbon; these data produced a large database for receptor modelling through Positive Matrix Factorisation (PMF). In the same period, a meteorological and air quality modelling system was implemented based on the mesoscale numerical weather prediction model WRF and the chemical transport model CAMx to obtain meteorological and pollutant concentrations up to a resolution of 1.1 km. The source apportionment was evaluated by CAMx over the same period that was used for the monitoring campaign using the Particulate Source Apportionment Technology tool. Even if the source categorisations were changed (i.e., groups of time-correlated compounds in PMF vs. activity categories in CAMx), the $PM_{2.5}$ source apportionment by PMF and CAMx produced comparable results. The different information provided by the two approaches (e.g., real-world factor profile by PMF and apportionment of a secondary aerosol by CAMx) was used jointly to elucidate the composition and origin of $PM_{2.5}$ and to develop a more general methodology. When studying the primary and secondary components of PM, the main anthropogenic sources in the area were road transportation, energy production/industry and maritime emissions, accounting for 40%–50%, 20%–30% and 10%–15%, of $PM_{2.5}$, respectively.

1. Introduction

The characterisation of emission sources is one of the most important issues affecting the assessment of efficient abatement strategies for PM pollution and the verification of their effectiveness. Anthropogenic and natural emissions contribute to PM levels, and these contributions can be highlighted through several source apportionment strategies. Receptor models (Gordon, 1988) reconstruct the contribution of each source by processing time series of PM compositional values that are measured at specific monitoring sites. However, because a mass balance equation must be resolved to identify and apportion sources of PM in the atmosphere, these

* Corresponding author.
E-mail address: prati@ge.infn.it (P. Prati).

http://dx.doi.org/10.1016/j.atmosenv.2014.05.039
1352-2310/

models can fail with reactive species and perform better in areas relatively close to the sources. Various approaches for source apportionment are currently available in the literature (Viana et al., 2008); each requires a different degree of *a priori* knowledge regarding the pollution sources. While the Chemical Mass Balance (CMB) model (Miller et al., 1972) requires a detailed chemical characterisation of the PM sources, multivariate models are useful when the information regarding the number and composition of the PM sources is scarce or absent. In this case, large data sets are required to obtain a reliable source apportionment. Positive Matrix Factorisation (PMF) (Paatero and Tapper, 1994) belongs to the latter category and has rapidly become a reference tool in this research field (e.g., Qin et al., 2006; Escrig et al., 2009; Contini et al., 2012; Cuccia et al., 2013).

Chemical Transport Models (CTMs) are a different approach; they are extensively used while investigating and assessing ambient air quality at various spatial and temporal scales (e.g., Russell and Dennis, 2000; Seigneur, 2001; Pirovano et al., 2012). Source apportionment tools are implemented in numerous models to understand the contributions from particular emission sources, specific processes, or individual chemical pathways to specific geographic receptor locations (Zhang et al., 2005; Wagstrom et al., 2008; Burr and Zhang, 2011). These tools also assess the formation of secondary aerosols because they apportion the gas precursor emissions.

Receptor and chemical transport models are rarely adopted with a synergic approach. This work describes a field experiment designed to compare and to integrate receptor models and CTMs. The study area is Genoa, Italy. Previous studies (Mazzei et al., 2008; Cuccia et al., 2013) provided profiles and apportioned the PM_{10}, $PM_{2.5}$ and PM_1 sources in several urban sites by processing the field data using only receptor models. The current experiment has been carried out as part of the MED-APICE project (http://www.apice-project.eu/); in this project, the Department of Physics of the University of Genoa evaluated the impact of harbour activities on the air quality. The monitoring activities were addressed to identify the major pollution sources and to set-up numerical tools that can reproduce the experimental results. During a dedicated field campaign, a near-complete characterisation of $PM_{2.5}$ was achieved, and significant amounts of data were collected in a large database for a PMF analysis. Simulations using the mesoscale Numerical Weather Prediction (NWP) model Weather Research and Forecasting (hereafter WRF; Skamarock et al., 2008) and the Eulerian CTM Comprehensive Air Quality model with Extensions (hereafter CAMx; ENVIRON, 2010) have been run over the entire monitoring period. The meteorological and pollutant concentration fields were obtained up to an approximately 1-km resolution. The source apportionment for $PM_{2.5}$ was evaluated by CAMx during the same period through a specific Particulate Source Apportionment Technology (PSAT) tool.

In this article, we introduce an integrated approach toward source apportionment techniques and their validation as a step toward a more general methodology.

2. Material and methods

2.1. Field equipment

The $PM_{2.5}$ samples were collected using low-volume samplers (Skypost by TRC TECORA), which were designed according to the CEN standards, at three sites (Fig. 1) selected based on the direction of the prevailing winds. Two sites (Corso Firenze and Multedo) are key nodes of the municipal air quality monitoring network; they are located immediately outside of the harbour area: the samplers were positioned with the inlets at approximately 3 m above ground. The third site was located in Bolzaneto, which is a northern district located approximately 7 km inland: the sampler was on a terrace approximately 12 m above ground. Briefly, Corso Firenze is in a residential area near a road with moderate traffic, the Multedo station lies along a private road with a very limited traffic, and the Bolzaneto station is located approximately 400 m from the highway connecting Genoa to Milan in a suburb with some industrial activities. The samplers were operated almost continuously and simultaneously from May 2011 to October 2011 with Teflon (PTFE, Pall: R2PJ047) and quartz fibres (Pallflex, 2500QAO UP) filter membranes (diameter = 47 mm, pore size = 2 μm). At each site, PTFE and quartz filters were alternated (i.e., one day PTFE was used, and quartz was used the next) every 24 h beginning at midnight. The number of collected samples was 122, 137 and 117, in Corso Firenze, Multedo and Bolzaneto, respectively.

Fig. 1. Map of the urban area of Genoa with the position of the three sampling sites.

2.2. Laboratory analyses

All filters were pre-conditioned for two days in a controlled room (temperature: 20 ± 1 °C, relative humidity: 50 ± 5%) before and after the sampling before being weighed using an analytical balance (sensitivity: 1 μg). The compositional analyses were conducted using different methods, depending on the characteristics of each filtering membrane. In particular, the PTFE filters are very clean and thin; therefore, they are ideal for compositional studies, including Energy-Dispersive X ray Fluorescence (ED-XRF) analyses (Ariola et al., 2006). They are also suitable for obtaining the ion concentrations via ion-chromatography (Chow and Watson, 1999). The quartz fibre filters can cause problems during elemental/chemical analyses due to their thickness, composition and internal contamination, but are required to determine the organic (OC) and elemental carbon (EC) through thermal-optical methods (Huntzicker et al., 1982; Chow et al., 1993). The quartz fibre filters were not treated before sampling; any possible contamination was assessed in each batch before sampling (maximum OC contamination was 1.7 ± 0.3 μg C cm^{-2}). Field blank filters were used to monitor any possible artefacts.

The elemental compositions of the $PM_{2.5}$ samples collected on both quartz and PTFE filters were measured by ED-XRF using an ED-2000 spectrometer by Oxford Instruments (Ariola et al., 2006). Before the field campaign, the $PM_{2.5}$ samples were collected side-by-side on Teflon and quartz fibre filters before the ED-XRF analyses: no discrepancies were observed between the elemental concentrations for elements heavier than K measured during the same day with the two collection membranes (Fig. E1 in the Electronic Supplementary Material, ESM). In addition, the S and K concentration values determined using ED-XRF in the PM collected on the quartz fibre filters were corrected for an average attenuation factor (Fig. E1) to determine their mean concentrations (more details in Table 1); this correction was not included in the PMF analysis. The water-soluble inorganic components of all of the samples were determined by ion chromatography (IC) using an ICS-1000 Ion Chromatography System (Dionex). The PM was extracted from the filters analysed previously by ED-XRF (or the portion remaining after the EC/OC determination, see below). A quarter of each filter had been wetted previously with 50 μL methanol; three successive extractions with MilliQ water of 20 min in an ultrasonic bath were required for a nearly complete recovery (approximately 98% ± 3%) renewing the water at each step. The extracts were analysed using IC to identify the major ionic species (i.e., Na^+, NH_4^+, K^+, Mg_2^+, Ca_2^+, Cl^-, SO_4^{2-}, NO_3^-) with an overall 10% uncertainty for the ionic concentrations. The possible systematic differences during the IC analysis of PM collected on PTFE and quartz fibre filters had been determined previously; these differences fell within the overall accuracy of the techniques (Cuccia et al., 2013). The MSA (methanesulphonic acid) concentrations were also obtained through IC.

The OC and EC fractions collected on quartz fibre filters were directly quantified using the Thermal-Optical Transmittance (TOT) method (Birch and Cary, 1996) with a SUNSET EC/OC instrument while following the EUSAAR_2 protocol (Cavalli et al., 2010).

Alternating the two filter media during sampling affected the laboratory analyses. Some low-Z elements (Na to P) were not quantifiable via ED-XRF on the quartz filters due to the X-ray self-absorption of the filter and the high Si concentration in the membrane. This lack of information was partially recovered via IC. Conversely, the EC and OC concentrations were directly measurable every other day. The missing EC values were recovered by analysing the PTFE filters with a Multi Wavelength Absorbance Analyser (MWAA) (Massabò et al., 2013). In this case, the average mass absorption coefficient was deduced in each site from a correlation study between the absorbance and EC measured using TOT in the sub-set of quartz fibre filters; afterwards, it was used to convert the absorbance measured for each PTFE sample to an equivalent EC concentration value (Massabò et al., 2013).

Table 1
$PM_{2.5}$ composition for the whole campaign (May–October 2011) in the three sites: Mean and standard deviation of concentration values are given in ng m^{-3} and have been calculated considering the samples (reported as percentage frequency, *F*) with concentration values above their Minimum Detection Limit (MDL) only. For some species (i.e. Na, Mg, K and Ca) both the total concentration by ED-XRF and the soluble fraction by IC are reported. Na Mg, Al, Si, P concentration values on Quartz filters affected by self-attenuation effects with ED-XRF, have been not included in the results whereas the values on PTFE filters only are reported here. Finally, concentration values for S and K measured by ED-XRF with Quartz fibre filters were recovered through average correction factors (1.7 and 1.4, respectively) and included in the data set.

	Corso Firenze (ng m^{-3})			Multedo (ng m^{-3})			Bolzaneto (ng m^{-3})		
	Mean	St. Dev	*F*	Mean	St. Dev	*F*	Mean	St. Dev	*F*
$PM_{2.5}$	13,113	4778	100%	12,657	4828	100%	14,031	5403	100%
Na	166	137	46%	197	175	52%	174	134	47%
Mg	39	21	46%	48	24	50%	45	32	46%
Al	40	49	51%	44	54	50%	48	48	49%
Si	112	108	50%	110	119	50%	151	127	49%
P	6	2	50%	7	2	50%	8	3	48%
S	1266	753	99%	1284	798	100%	1367	745	100%
K	95	55	97%	86	52	99%	172	188	100%
Ca	88	55	99%	68	38	98%	123	188	100%
Ti	7	4	80%	7	4	83%	17	25	92%
V	15	11	91%	14	11	91%	10	5	89%
Mn	4	3	77%	5	5	81%	109	209	91%
Fe	120	55	99%	111	55	98%	524	783	99%
Ni	7	4	95%	6	4	92%	5	3	89%
Cu	6	5	96%	4	2	93%	28	36	99%
Zn	16	12	94%	20	17	96%	74	121	98%
Br	4	2	93%	4	2	96%	4	2	97%
Mo	4	4	48%	2	1	46%	3	2	49%
Pb	5	3	79%	6	5	75%	28	72	92%
OC	2463	1140	100%	2148	1294	100%	2163	1129	100%
EC	1340	686	100%	904	343	100%	1503	725	100%
MSA	80	138	53%	60	43	50%	50	37	49%
Cl^-	36	28	51%	45	64	57%	36	31	58%
NO^{3-}	325	644	84%	207	216	67%	244	229	74%
SO_4^{2-}	3770	2011	98%	3759	2106	99%	3307	1890	100%
Na^+	222	336	49%	268	201	76%	201	157	67%
NH_4^+	1419	730	100%	1376	767	100%	1175	720	100%
K^+	58	42	75%	70	52	86%	115	144	91%
Mg^{2+}	34	22	100%	38	27	100%	40	25	100%
Ca^{2+}	79	63	60%	63	40	61%	105	174	67%

2.3. Receptor model-PMF

The PMF methodology was described by its developers (Paatero and Tapper, 1994; Paatero, 1997). The important advantage of PMF is its ability to handle missing data, values below the detection limits and outliers by adjusting the error estimates of each data point. In this work, the PMF2 program (Paatero, 2010) was used in robust mode to reduce the influence of any numerical outliers.

The PMF analyses were carried out separately using the data sets from each sampling site. The variables were selected according to the signal-to-noise criterion (Paatero and Hopke, 2003), and 18 variables were finally retained during the analyses: Al, Si, K, Ca, Ti, V, Mn, Fe, Ni, Cu, Zn, Pb, SO_4^{2-}, NO_3^-, NH_4^+, Na^+, OC and EC. The number of samples considered in the PMF runs (122, 134 and 114, in Corso Firenze, Multedo and Bolzaneto, respectively) is sufficient for an accurate source apportionment study (Thurston and Spengler, 1985). All of the concentration values and their associated errors were treated according to Polissar et al. (1998). The OC missing values, which correspond to the PM samples collected on the PTFE filters, were calculated from the EC concentration values measured in each sample by the MWAA and adopting the mean OC to EC ratio

measured using the sub-set of quartz filters sampled at the same site. These estimated OC concentration values were included in the PMF data sets as missing data and, according to Polissar et al. (1998), with a large uncertainty (400% relative error). Similarly, the missing Al and Si concentration values, which correspond to PM samples collected on the quartz fibre filters, were treated as missing data by adopting the mean values measured with the subset of PTFE filters sampled at the same site and applying a 400% uncertainty. The procedure was tested by running the PMF with the entire data set and with a sub-set containing only the quartz filter samples: this procedure produced globally well-compatible results in terms of the factor numbers, profiles and apportionment (see Section 3.3 and details on $PM_{2.5}$, OC and EC in Table E1 in ESM). Because PMF is affected by the rotational ambiguity (Lee et al., 1999; Paatero et al., 2002), it directly implements rotations in the minimisation algorithm controlled using the FPEAK parameter (Paatero, 1997). The best rotation for each factor was chosen in the FPEAK range from -2 to $+2$ while discarding the rotations that correspond to profiles without physical meaning (i.e., the sum of elemental concentrations exceeded 100%) and selecting those generating concentration ratios between the tracer elements of the natural sources (e.g., crustal matter) that are comparable to the literature values. To consider the effect of the rotational ambiguity, we used the standard deviation calculated for the rotations (i.e., for each element, the distribution of its weights in the factor profiles corresponding to different rotations) to reveal the variability of factor profiles (Mazzei et al., 2008; Cuccia et al., 2010).

2.4. The chemical transport model setup

The source apportionments were also obtained through an integrated air quality forecasting system, which was implemented while the $PM_{2.5}$ sampling campaign was underway. The meteorological fields were provided by the non-hydrostatic mesoscale model WRF-ARW (Skamarock et al., 2008), version 3.2.1, while the air quality simulations were performed using the photochemical dispersion model CAMx (ENVIRON, 2010).

Three nested computational domains in a Lambert Conic Conformal projection were defined for the WRF model, which covered Western and Central Europe with a 10-km horizontal resolution, Northern Italy with a 3.3-km horizontal resolution and the urban area of Genoa with a grid spacing of 1.1 km (Fig. 2). Thirty-five terrain-following vertical levels were adopted, with higher resolutions closer to the surface. The topography, land use and land-water mask data sets for the aforementioned domains were interpolated from the 5′-, 2′- and 30″-resolution USGS data sets, respectively. A full set of well-known and widely used physical parameterisation schemes was adopted. For the long-wave radiation, the Rapid Radiation Transfer Model (RRTM) scheme (Mlawer et al., 1997) was selected, while for the short-wave solar radiation, the Goddard scheme (Chou and Suarez, 1994) was adopted. The Kain-Fritsch parameterisation (Kain, 2004) was used for the cumulus (in the parent domain only, while in the higher-resolution domains, the convection could be explicitly resolved), the Mellor-Yamada-Janjic (MYJ PBL) scheme (Janjic, 2002) was used for the boundary layer, and the Thompson scheme (Thompson et al., 2008) was used for the microphysics. Finally, the Eta similarity surface layer scheme (Janjic, 2002) and the Noah land surface model (Chen and Dudhia, 2001) were adopted.

The initial and boundary conditions for the atmospheric simulations with WRF were generated from the operational global model GFS (Environmental Modeling Center, 2003) outputs ($0.5^\circ \times 0.5^\circ$ resolution). Twenty-four-hour-long WRF simulations were performed while saving the outputs every hour and updating the analysis every 24 h; the boundary conditions were upgraded every three hours. This type of approach generates unavoidable discontinuities in the simulated fields every 24 h. However, these discontinuities are a minor drawback in the present context; their influence on the concentration fields is reasonably small due to the delayed response to meteorological forcing.

CAMx is a Eulerian chemistry transport model that includes gas and aerosol chemistry, wet and dry deposition processes, aqueous phase processes, thermodynamic partitioning of the inorganic aerosols and secondary organic aerosol formation/partitioning. Particulate matter Source Apportionment Technology (PSAT) has been implemented in the CAMx model and is publicly available (Wagstrom et al., 2008; ENVIRON, 2010). The PSAT estimates the contributions of specific emissions source groups, emissions source regions, initial and boundary conditions to the PM using reactive tracers. The PSAT tracks the contributions to mercury and PM sulphate, nitrate, ammonium, secondary organic aerosol, and inert species. Nonlinear processes, including gas and aqueous phase chemistry, are solved for bulk species and apportioned to the tagged species.

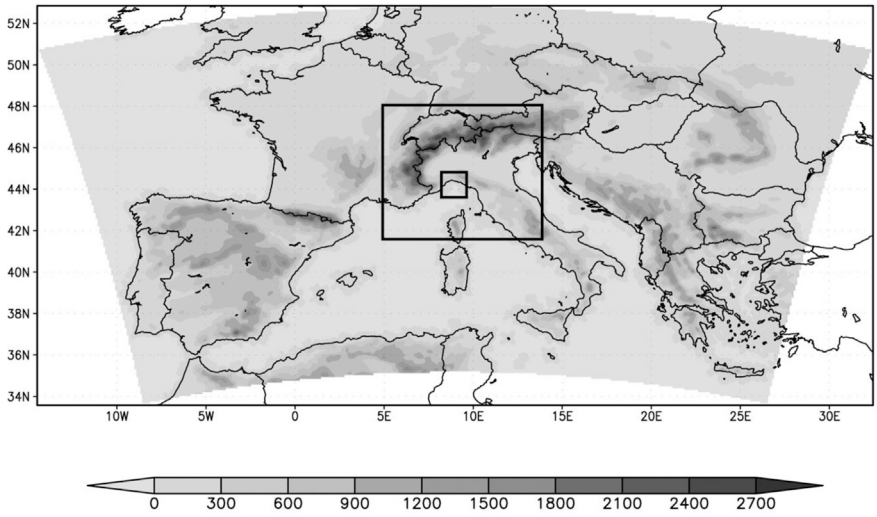

Fig. 2. Topography (m) of the outermost WRF computational domain and location of the nested domains: Western and Central Europe (grey area), Northern Italy (larger box) and the urban area of Genoa (smaller box). For CAMx simulations the outermost and the innermost domain only have been used.

In this study, we used CAMx version 5.2 with the Carbon Bond 2005 (CB05) gas phase chemistry mechanism (Yarwood et al., 2005). The PPM advection solver by Colella and Woodward was used to determine the horizontal advection (Odman and Ingram, 1993), while a simple K-theory approach was used to describe the turbulent vertical diffusion. Hertel's EBI solver was adopted to solve the gas-phase evolution over time (Hertel et al., 1993), while the aerosol chemistry was described using a coarse-fine (CF) scheme. To limit the computing time, only two 2-way nested CAMx modelling domains were defined: an outer domain with a 10-km horizontal resolution and an inner domain coincident with the 1.1-km resolution WRF finest domain (Fig. 2). Sixteen vertical levels were defined, and the ten lowest CAMx layers matched the WRF layers exactly; the surface layer was approximately 30 m above the ground.

The large-scale anthropogenic emissions data for gaseous (NO_x, SO_x, NH_3, CO, NMVOCs) and particulate (PM_{10}, $PM_{2.5}$) pollutants were provided by the Aristotle University of Thessaloniki (AUTH) after processing the 2005 European data set collected by The Netherlands Organisation (TNO) with the MOSESS (MOdel for the Spatial and tEmporal diStribution of emissionS) code (Markakis et al., 2013). MOSESS is designed to create model-ready emission inventories and is capable of handling temporal disaggregation (annual/daily and diurnal processing), chemical speciation of the NMVOCs and particles, vertical distributions and point source treatments, as well as the spatial disaggregation of the emissions, by utilising numerous spatial proxies including high-resolution land uses.

High-resolution (1 km) gridded emission data were obtained from the Liguria Region inventory for the reference year 2008 (with harbour emissions updated to 2010). Finally, the biogenic and natural emissions (Isoprene, Monoterpenes, biogenic other NMVOCs, sea salt and wind-blown dust) were computed from the WRF outputs using the NEMO (Natural Emission MOdel) model, developed by AUTH (Poupkou et al., 2010).

3. Results

3.1. $PM_{2.5}$ composition

In Table 1, the average $PM_{2.5}$ compositions of the three sites are reported. The $PM_{2.5}$ levels were very similar, exhibiting high regression coefficients among their concentration time series ($R^2 = 0.7$ and 0.5 for time series of Multedo and Bolzaneto vs. Corso Firenze, respectively, slope $\sim$1 in both cases). The concentration time series for the major $PM_{2.5}$ components (see Table 1) were even more highly correlated; the regression coefficients for SO_4^{2-} ($R^2 \sim 0.8$), NH_4^+ ($R^2 \sim 0.8$) and OC ($R^2 \sim 0.7$) were high, and the slopes were always approximately 1. Instead, EC showed larger variability with higher concentrations in the sites exposed to intense vehicular traffic (i.e., Corso Firenze and Bolzaneto, see Table 1).

The mean concentration ratios for $S:SO_4^{2-}$ (0.4 ± 0.1, 0.4 ± 0.2, 0.4 ± 0.2 in Corso Firenze, Multedo and Bolzaneto, respectively) and $SO_4^{2-}:NH_4^+$ (2.7 ± 0.9, 2.7 ± 1.0 and 2.7 ± 1.0 in Corso Firenze, Multedo and Bolzaneto) indicated that the sulphur in $PM_{2.5}$ was almost exclusively in the sulphate form; furthermore, $(NH_4)_2SO_4$ was the more abundant inorganic secondary compound (see Table 1), accounting for approximately 40%, 41% and 32% of the $PM_{2.5}$, in Corso Firenze, Multedo and Bolzaneto, respectively. The MSA concentration values can be used to roughly estimate the fraction of SO_4^{2-} due to biogenic activities through the relation described by Bates et al. (1992): when assuming the average ambient temperature is 22 °C, the mass ratio was 0.09 for $MSA:SO_4^{2-}$; SO_4^{2-} refers to the sulphate formed after oxidising dimethylsulphide. Considering that the MSA concentrations were above the MDL in approximately 50% of samples, Table 1 reveals that the biogenic sulphate could be estimated to account for less than 10% of the total SO_4^{2-}. According to the measured Na concentrations and the $Na:SO_4^{2-}$ concentration ratios in the seawater (Seinfeld and Pandis, 1986), the fraction of sulphate with a marine origin was even smaller (<1%), indicating that the measured ammonium sulphate concentrations had a near-exclusive anthropogenic origin.

3.2. CTM validation

The modelling system was thoroughly validated versus the meteorological (Fig. E2 in ESM) and air quality observational data. The concentration values predicted by CAMx have been compared to the results of the $PM_{2.5}$ monitoring campaign and data from the municipal air quality monitoring network (PM and gaseous pollutants). In Fig. 3, the time series for the predicted and measured daily $PM_{2.5}$ concentrations in the three monitoring sites are shown.

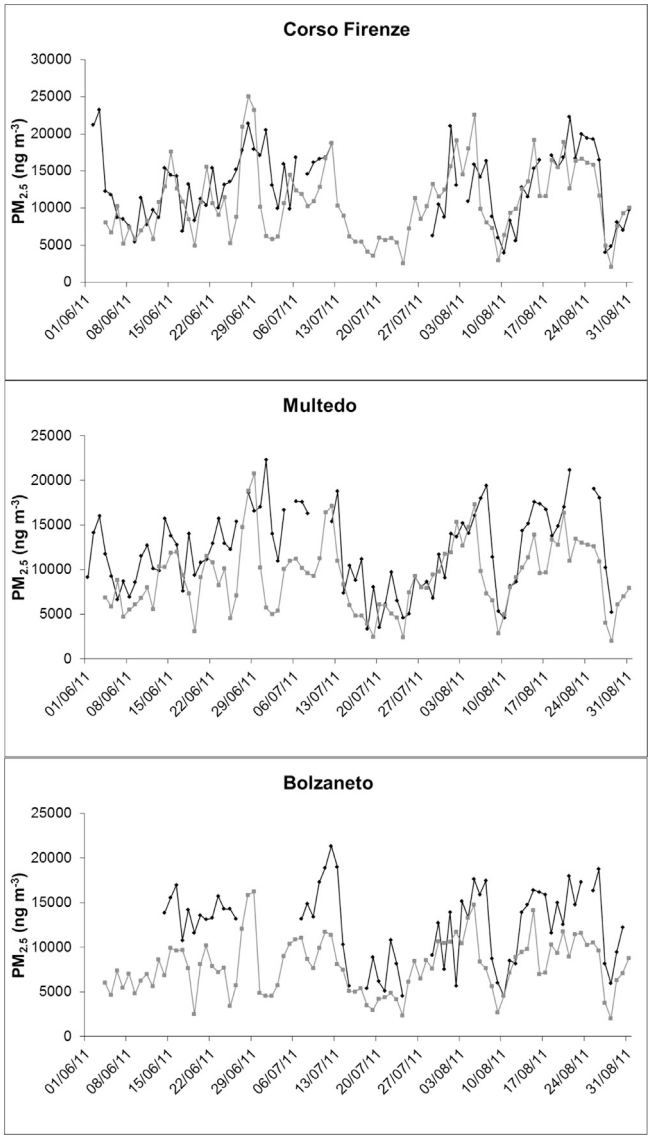

Fig. 3. Time series of predicted (grey) and measured (black) daily $PM_{2.5}$ concentration values in the three monitoring sites. Missing data are due to technical problems during the sampling.

A bilinear interpolation was used to compute the concentrations at the exact locations of the sampling stations. The model predictions reproduced the observational data satisfactorily in terms of magnitude (though a tendency toward slight underestimation appeared, particularly at Bolzaneto) and evolution over time. The correlation values and regression results were comparable with the outcomes of the other studies conducted throughout Europe and Northern Italy (see Table E2 in ESM and the references therein).

In Fig. 4 (top and central panels), the time series for the predicted and measured sulphate and ammonium daily concentrations at the three monitoring sites are presented. Despite some local discrepancies that lowered the correlation values (Table E2), the overall agreement is remarkable, revealing that the model could reproduce the major components of the $PM_{2.5}$ and adequately describe the processes leading to the formation of secondary sulphates. In contrast, the agreement is quite poor for secondary nitrate, as shown in Fig. 4 (bottom panels). This mismatch is consistent with an analogous comparison of NO_x concentration data, revealing that the model cannot reproduce NO_x chemistry (in particular NO) properly or that the emission inventory is inaccurate.

Finally, even though the model for the OC tends toward underestimation, the predictions and measurements agree (Fig. 5, upper panels), especially at Bolzaneto (see also Table E2). The measured EC concentration values are poorly reproduced by CAMx; the model tends toward overestimation, and a lower correlation is apparent between the predicted and observed evolution over time, particularly at Corso Firenze and Multedo (Fig. 5, lower panels).

3.3. Source apportionment by PMF

The PMF analysis was performed separately for the three data sets; however, five factors were resolved everywhere and labelled according to their characteristic tracers (Viana et al., 2008): *Traffic* (Cu, Zn, Pb), *Soil Dust* (Al, Ti), *Heavy Oil Combustion* (V, Ni), *Secondary Sulphates* (SO_4^{2-}, NH_4^+), and *Secondary Nitrates* (NO_3^-).

Sea salt, which was observed quantitatively in $PM_{2.5}$ during previous studies in the same area (Cuccia et al., 2013), was not resolved in this experiment because Cl was not included in the PMF analysis, and the Na was associated with the NO_3^- (see discussion below). The MSA concentration values were often below the MDL and were not included in the PMF data set, preventing the resolution of the biogenic PM. In addition, the biomass-burning tracers were not resolved during the laboratory analyses, and a factor attributable to Secondary Organic Aerosols was not identified by PMF. Additional "local" sources have been singled out by PMF in some sites, but a discussion of their profiles is beyond the scope of this work: their small contribution to the $PM_{2.5}$ levels is shown in Table 2.

The PMF profiles of the five common factors are reported in Fig. 6.

The average concentration ratio for SO_4^{2-}:NH_4^+ in the *Secondary Sulphates* factor was 2.9 ± 0.1, which is consistent with the stoichiometric ratio for $(NH_4)_2SO_4$.

In the coastal regions, *Secondary Nitrates*, which were traced by NO_3^-, can be linked to the formation of NH_4NO_3 and $NaNO_3$ (Cuccia et al., 2013); the concentration ratio for Na:NO_3^- in the *Nitrates* profile are consistent with the $NaNO_3$ stoichiometry at two sites (Corso Firenze and Bolzaneto).

The *Heavy Oil Combustion* factor profiles obtained at the three sites are characterised by an average V:Ni concentration ratio of 2.8 ± 0.3, agreeing with the city mean of V:Ni = 3.0 ± 0.7 (Mazzei et al., 2008). These profiles present a high concentration of SO_4^{2-} and NH_4^+ (average SO_4^{2-}:NH_4^+ concentration ratio = 3.8 ± 0.6, enriched in sulphates relative to the *Secondary Sulphates* factor); the presence of NH_4^+ is likely due to the incomplete separation of the major sources during the PMF analysis.

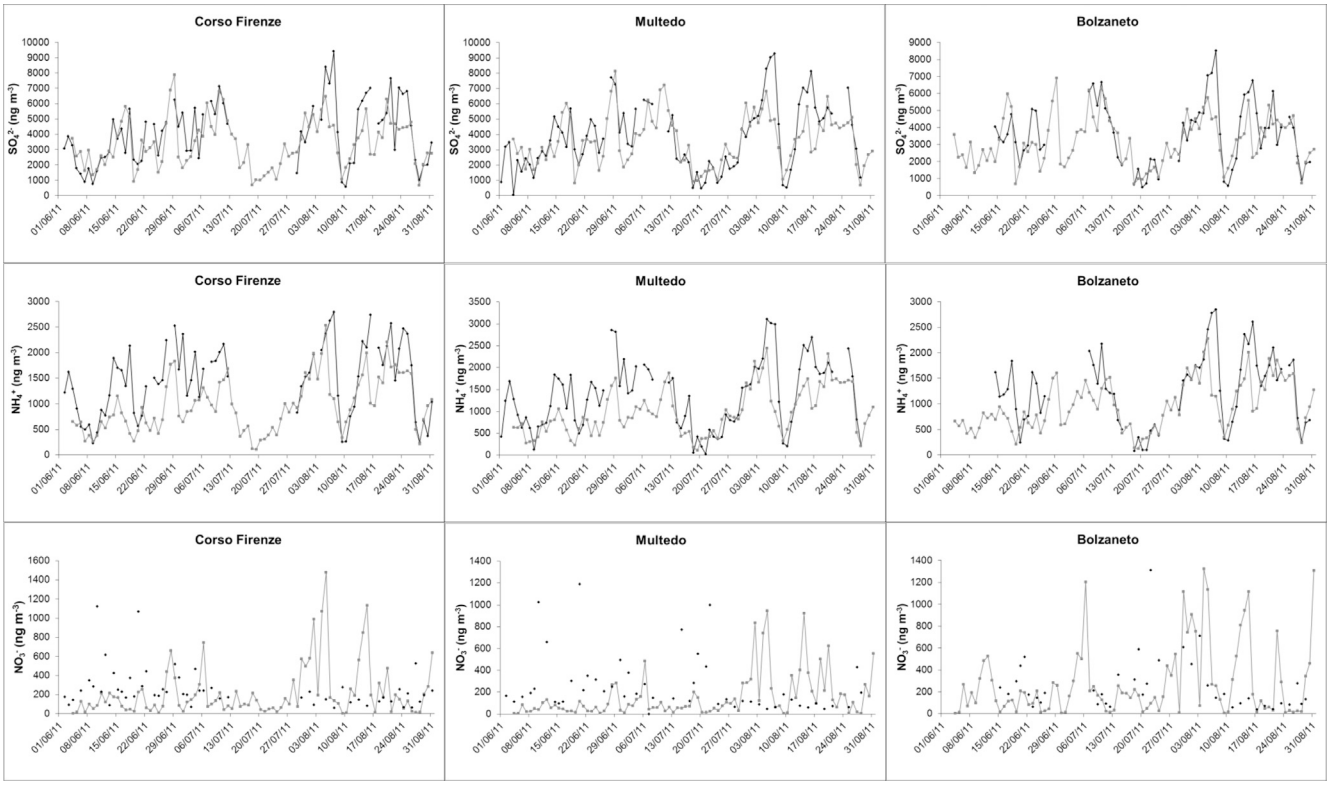

Fig. 4. Time series of predicted (grey) and measured (black) SO_4^{2-}, NH_4^+ and NO_3^- concentration values (daily averages) in the three monitoring sites.

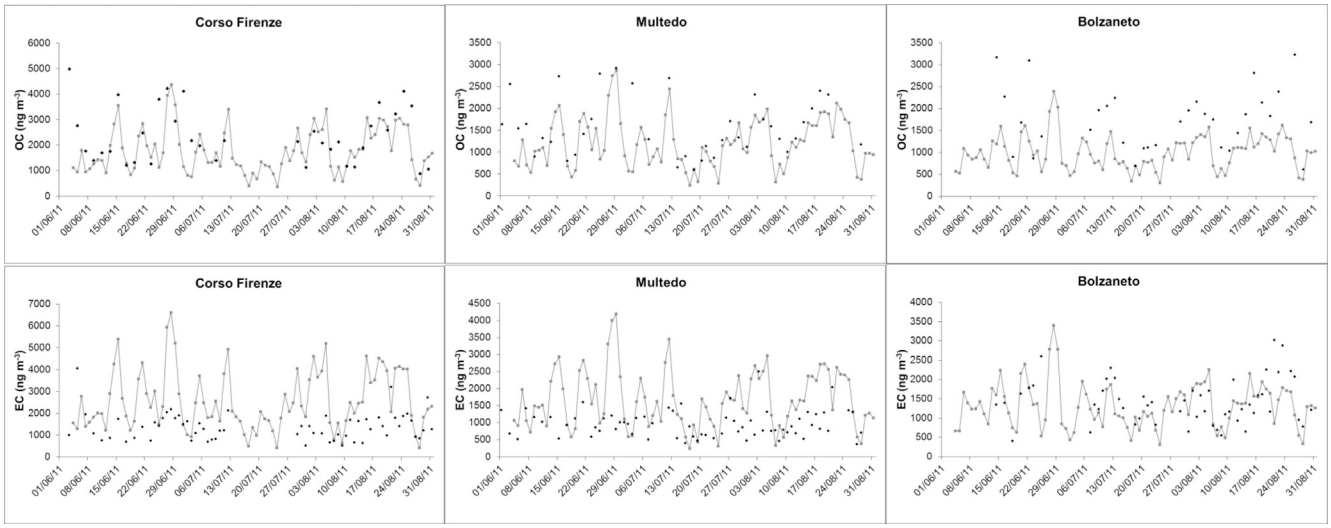

Fig. 5. Time series of predicted (grey) and measured (black) daily-averaged OC and EC concentration values in the three monitoring sites.

In the *Traffic* factor, the average concentration ratios of the tracer elements were as follows: Cu:Pb = 1.6 ± 0.5 and Cu:Zn = 0.45 ± 0.05. These values are comparable to those measured previously (Mazzei et al., 2008; Cuccia et al., 2013) in Genoa. The average ratio between the OC and EC was 1.5 ± 0.3, which is consistent with the literature values for $PM_{2.5}$ (Ho et al., 2006).

The *Soil Dust* factor profiles are characterised by average Al:Si and Al:Ca ratios of 0.43 ± 0.04 and 1.9 ± 0.5, respectively, which are comparable to the average figures (0.3 and 2, according to Mason, 1966).

The profiles of the five factors separated in the three sites showed different levels of similarity. The *Sulphates* profile was very comparable, as shown in Fig. E3 in ESM ($R^2 \sim 1$). *Traffic* and *Soil Dust* had very highly correlated profiles in the three sites ($R^2 \sim 1$ and 0.9, respectively for *Traffic* and *Soil Dust*). The *Nitrates* and *Heavy Oil Combustion* profiles were different between Corso Firenze and the other sites; we obtained very similar figures for Multedo and Bolzaneto ($R^2 \sim 0.8$ and 1, respectively for *Nitrates* and *Heavy Oil Combustion*).

In Table 2, the average $PM_{2.5}$ apportionment in the three sites is compared. The major components of $PM_{2.5}$ were secondary inorganic compounds (on average: *Sulphates* ~50%, *Nitrates* ~7% of $PM_{2.5}$, respectively) with very similar percentages across the three sites. The concentration of ammonium sulphate, as deduced by the raw statistics given in Table 1, was approximately 30%–40% of $PM_{2.5}$ at each site (see section 3.1). The difference between this percentages and the figure obtained through PMF (~50% of $PM_{2.5}$) can be almost completely ascribed to the OC contamination present in the *Sulphates* profiles (see Fig. 6): this contamination ranges from 10% to 20% of the *Sulphates* mass, and therefore from 20% to 40% when assuming a OM:OC ratio (OM = Organic Matter) of 1.8, which is typical of aged organic aerosols (Favez et al., 2010). A similar consideration holds for the *Nitrates* factor; these profiles include sea-spray elements (approximately 15%, Fig. 6) and carbonaceous compounds (approximately 20%, Fig. 6). *Traffic* affected every site as the major source of $PM_{2.5}$, while the variability was related to the location (~27%, 22% and 18% of $PM_{2.5}$, respectively in Bolzaneto, Corso Firenze and Multedo). The effect of *Heavy Oil Combustion* on $PM_{2.5}$ was higher in the sites closer to the harbour, but still significant at the inland site (~13%, 11% and 9%, respectively in Corso Firenze, Multedo and Bolzaneto). No major resident sources (e.g., oil-fuelled power plant) were active in the area, and the ship emissions were likely the predominant source of *Heavy Oil Combustion*. The seasonal trends in the passenger traffic in the harbour (Fig. E4 in ESM) support these results; an increase occurs in the summer when many ferries connect Genoa to tourism destinations in the Mediterranean Sea.

The apportionment of single elements and compounds is given in Fig. 7. Notably, the SO_4^{2-} and NO_3^- concentrations were mainly associated with the *Secondary Sulphates* and *Nitrates* (on average 82% and 80%, respectively). NH_4^+ was primarily associated with one of the secondary components of $PM_{2.5}$ (on average: 86% in *Sulphates*). Approximately 60% of the EC was attributed to *Traffic*, 25% was attributed to *Heavy Oil Combustion* and the remainder was shared among the other factors. The figure is slightly different for OC, the concentration of which was attributed for approximately 50%, 40%, and 10%, respectively, to the *Traffic*, *Secondary Sulphates*, and *Secondary Nitrates*.

Table 2
Average source apportionment obtained by the PMF analysis of the $PM_{2.5}$ data sets collected during the whole campaign (May–October 2011) in the three sites. The contributes of the two different local sources singled out in two sites are also reported.

	Corso Firenze (ng m^{-3})	Multedo (ng m^{-3})	Bolzaneto (ng m^{-3})
Traffic	2860 ± 310	2190 ± 300	3970 ± 570
Heavy Oil Combustion	1710 ± 260	1410 ± 210	1290 ± 140
Nitrates	780 ± 140	890 ± 160	1140 ± 230
Sulphates	6500 ± 450	6460 ± 620	6770 ± 590
Soil Dust	880 ± 180	870 ± 140	810 ± 210
Local Source	–	560 ± 100	670 ± 460

3.4. Source apportionment by CAMx-PSAT

The source apportionments for PM_{10} and $PM_{2.5}$ have been evaluated by CAMx over two periods: Summer (June–August 2011) and late Autumn (November, 15–December, 15 2011). The apportioned categories have been defined following the SNAP declaration (Selected Nomenclature for Air Pollution) sectors (EEA, 2009) and have been chosen according to an analysis of the local emission inventory, in which sources expected to have high impacts on the air quality in Genoa can be identified. In particular, five PM source

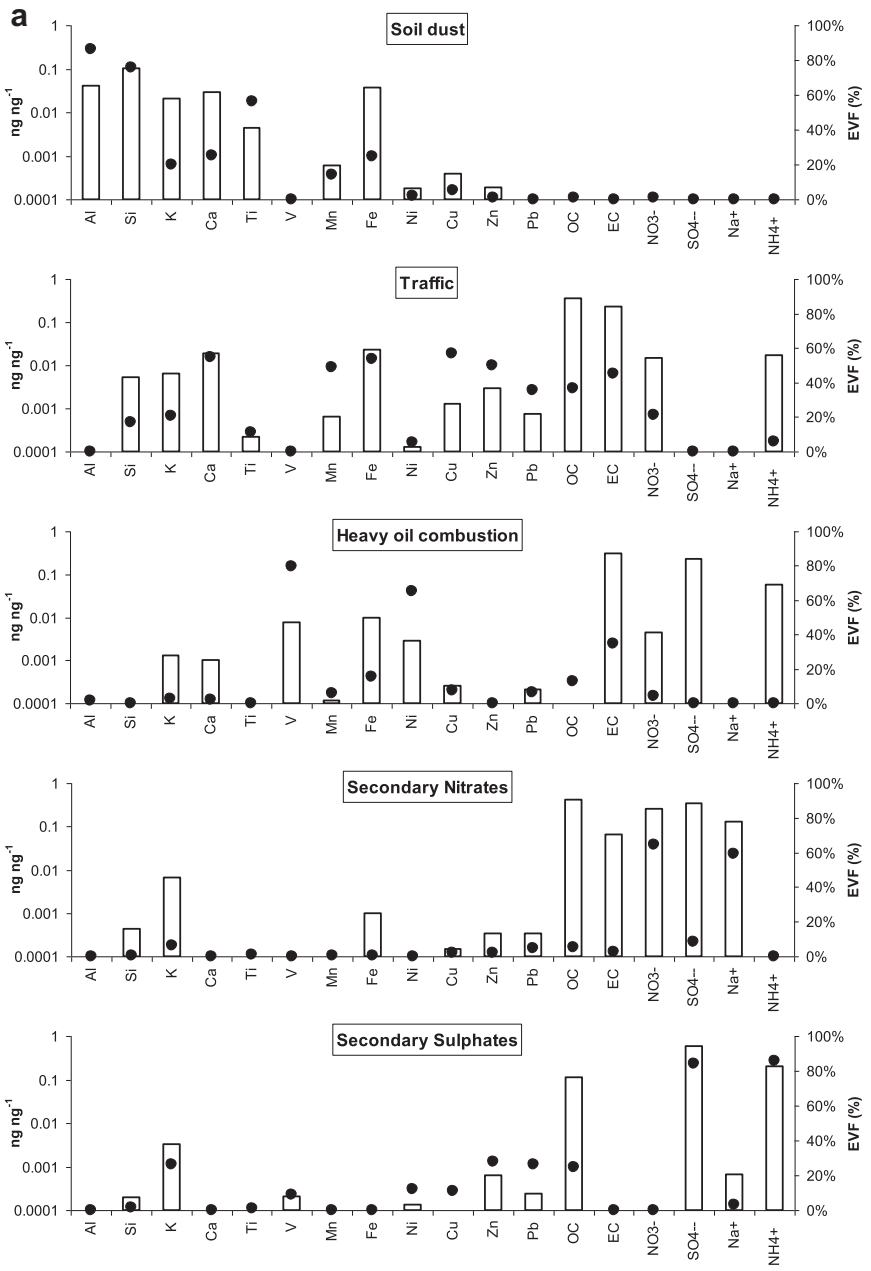

Fig. 6. PMF profiles (left axis, white bars) and evaluation factors, EVF (right axis, black circles) of the $PM_{2.5}$ sources resolved in all the sampling sites: a) Corso Firenze, b) Multedo, c) Bolzaneto.

categories were considered: Maritime and Harbour activities (SNAP code 0804), Road Transport (SNAP code 07), Energy production – Industry (SNAP codes 01, 03, 04), Non-industrial combustion plants (SNAP code 02, in Genoa area mainly residential sources, hence labelled as "Residential" hereafter) and Other sources (including boundary conditions). Even if the PSAT results are available for the entire domain, the source apportionment outcomes are here focused for the three sites where the $PM_{2.5}$ monitoring campaign was performed: Corso Firenze, Multedo and Bolzaneto.

In Table 3, we report the average of the predicted contributions of the listed sources to the $PM_{2.5}$ levels in the two periods. The primary impact is related to road traffic, and the minor contributions are provided by industrial and maritime activities. A seasonal trend can be identified in both the coastal and inland sites. During the winter, a strong increase in the contribution of the "Residential" sources is observed, which can be ascribed to the presence of residential heating emissions. Moreover, in the coastal sites, a strong reduction in the contribution of maritime activities is observed because the passenger traffic in the harbour is much lower than during the summer. The maritime contributions to $PM_{2.5}$ vary among the three sites: between 4% and 11% in the summer and decreasing to 3%–5% in the winter.

3.5. Source apportionment comparison: PMF vs. CAMx-PSAT

The $PM_{2.5}$ apportionment obtained through the two approaches (i.e., PMF and CAMx-PSAT) was compared for the period shared by the two data sets, i.e., June–August 2011. For PMF, we extracted the factor profiles while processing the entire data sets; we calculated

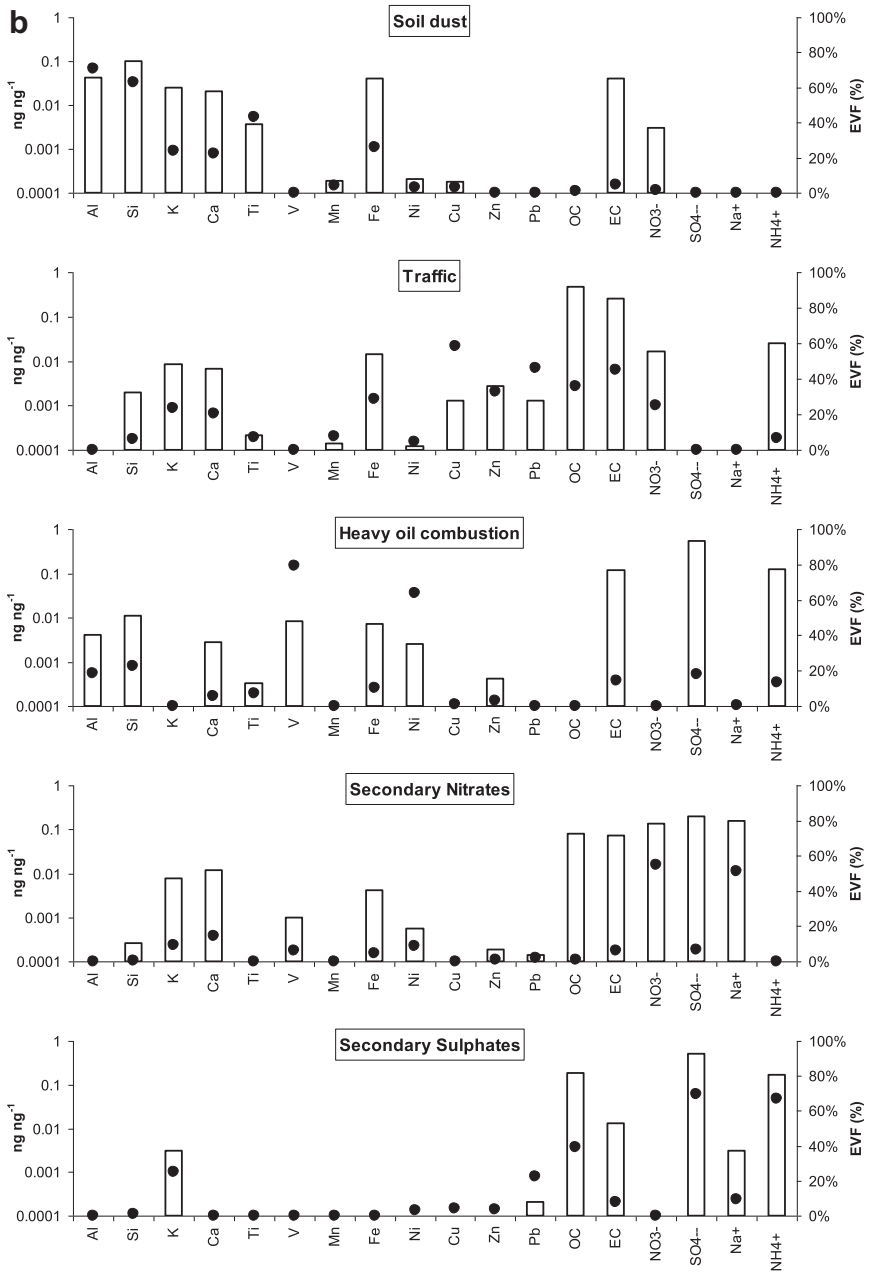

Fig. 6. (*continued*).

the average $PM_{2.5}$ apportionment for the overlapping three months only. This comparison caused two major problems:

a) The methods used to single out PM sources are completely different: with the receptor model approach, a "source" ("factor", with the PMF terminology) is essentially a group of PM components for which the concentration values remain constant over time or, alternately, show correlated time trends. The identification of the sources by the CTMs is based on the structure of the emission inventory categories, which is defined by the user through a bottom-up approach with each activity associated with a specific emission pattern.
b) The secondary PM components are resolved and treated similarly to the other primary PM sources in the receptor model approach (i.e., they have a specific profile that corresponds to a certain fraction of the whole PM); with CTMs, the impact of each source/activity on the PM level is calculated to include both the primary and secondary components of the emission pattern; therefore, the CTM does not and cannot resolve any type of "secondary" source for comparison with a PMF factor.

When trying to overcome these two problems, we rearranged the $PM_{2.5}$ sources singled out by PMF and considered the factor profiles given in Fig. 6 to redistribute the PM associated to *Secondary Sulphates* and *Nitrates* to the other primary sources. While following the arguments provided in Section 3.3, we subtracted the OM contamination (which turned out to be in the June–August period ~20%, ~36% and ~22% of the *Sulphates* mass, in Corso Firenze, Multedo and Bolzaneto, respectively) from the $PM_{2.5}$ mass attributed by PMF to *Sulphates*, and we added the same amount to the *Traffic* impact, as suggested by the mean OC apportionment discussed in Section 3.3 (i.e., the only primary source that

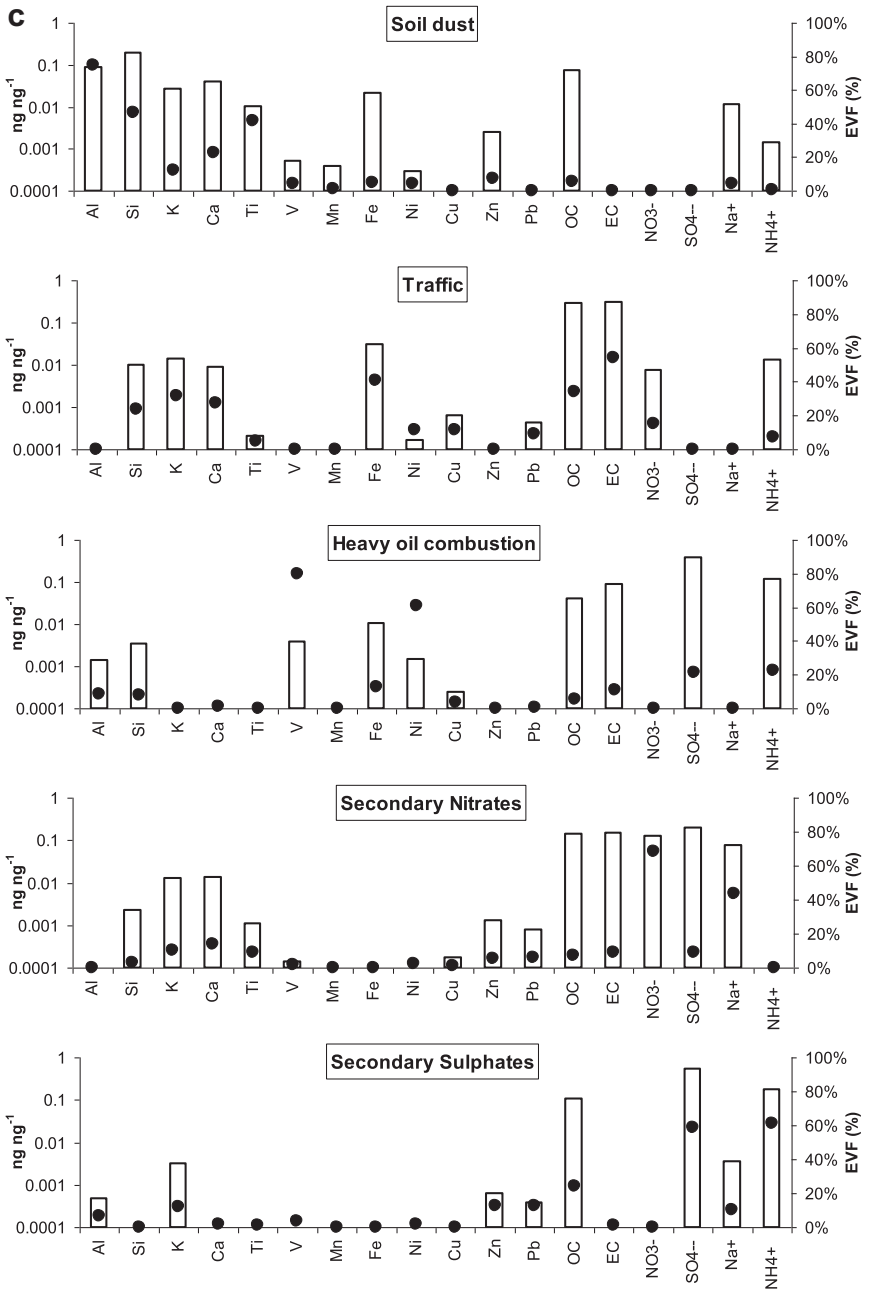

Fig. 6. (*continued*).

contributed to the OC concentration significantly was *Traffic*). Consequently, we neglected a possible OC regional background generated by the other PM sources: conservatively, we attributed a large uncertainty (i.e., a percentage error of 50%) to the PM amount "moved" from *Sulphates* to *Traffic*. With this correction, we attempted to redistribute the secondary organic aerosol to the primary processes that introduce OC into the atmosphere, even with a very crude approximation that charges the entire budget to *Traffic*. While using the same approach, we redistributed the mass attributed to *Nitrates* by PMF: in this case, we processed the data by sharing the *Nitrates* mass between the *Traffic* (6:10), *Heavy Oil Combustion* (3:10) and natural sources (1:10, sea spray). The sharing process was suggested by the factor profiles in Fig. 6 and by the average *Traffic* to *Heavy Oil Combustion* apportionment (approximately 2:1, see Table 2); it was adopted with a 50% uncertainty on each correction factor. Furthermore, approximately 10% of the *Secondary Sulphates* were attributed to the biogenic emissions quoted in Section 3.1: this mass was included in the *Other Sources* that were collectively sized by the CAMx-PSAT.

Finally, the source names were unified to the PSAT classification: *Traffic* was renamed *Road Transport*, *Heavy Oil Combustion* was treated as entirely related to the *Maritime* sector, the remaining *Sulphates* (i.e., after the corrections above described) were included in the *Energy Production – Industry* sector (according to the emission inventory, the 340 MW coal-fuelled power plant located in the harbour area was the major source of SO_x and sulphates in the study area). This approximation is quite crude because part of the *Secondary Sulphates* concentration might be attributed to other source categories (in particular: the relative SO_4^{2-} concentration in the *Heavy Oil Combustion* profile could not incorporate the total

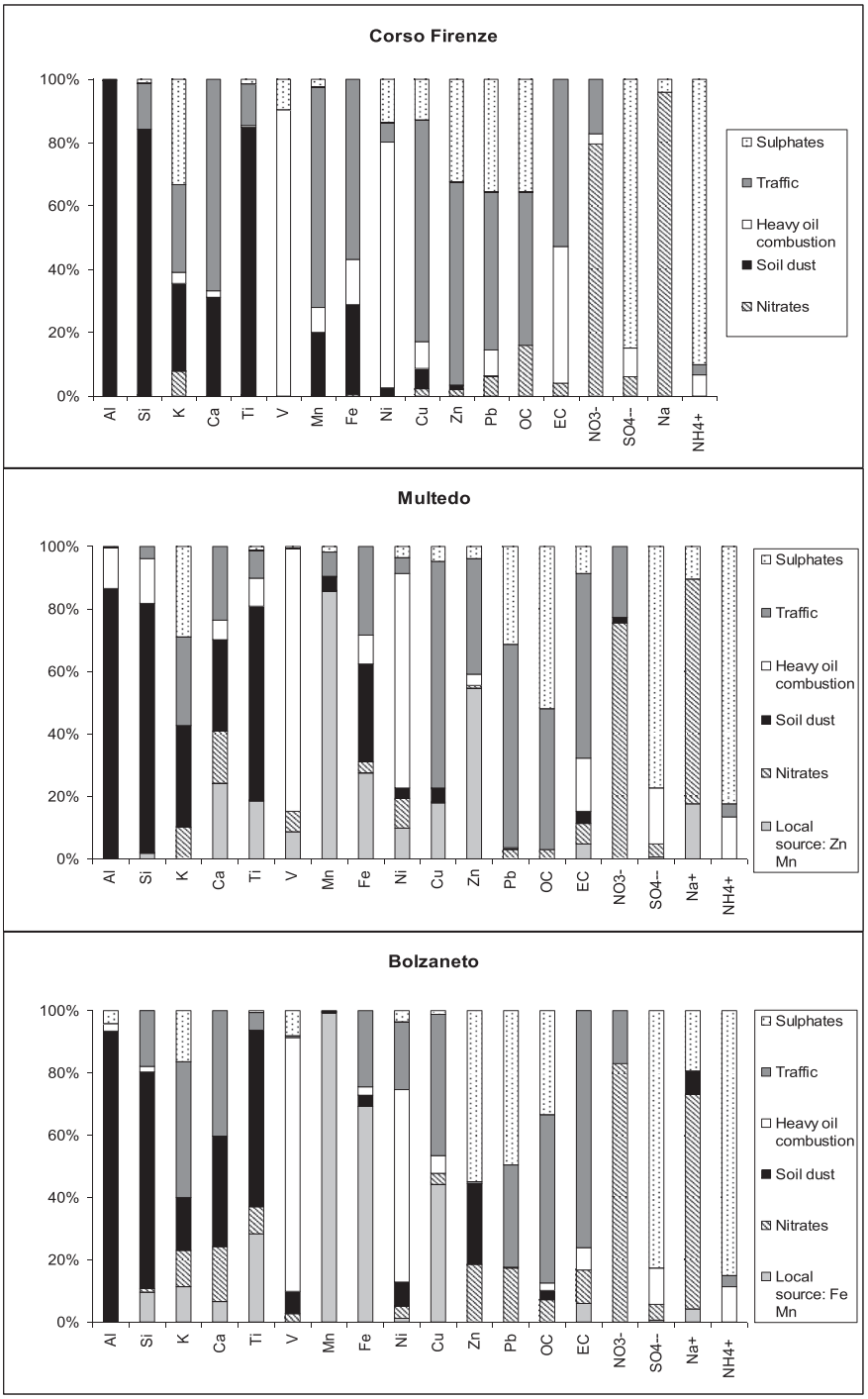

Fig. 7. Average apportionment of elements/compounds concentration in each sampling site calculated with the $PM_{2.5}$ data sets of the whole field campaign (May–October 2011). The contributes of the two local sources singled out in Multedo and Corso Firenze, likely related to specific industrial activities, are also reported.

secondary PM attributed to ship emissions). Therefore, the figure obtained for *Energy production – Industry* (see below) should be considered an upper limit. However, because CAMx predicted the trends in the SO_4^{2-} and NH_4^+ concentrations over time with considerable accuracy (see Fig. 4), we considered our approximation reasonable. *Soil Dust* and the "local" sources resolved in some sites were added and labelled with the natural *Sulphates* and *Nitrates* sources as *Other sources*.

The results of this exercise are provided in Table 4: the overall picture moderately agrees with the apportionment obtained by CAMx-PSAT. The PSAT underestimated the maritime emissions; this underestimation might be due to the missing contributes of ships emissions approaching the harbour because the regional source inventory does not include this information. However, the *Other sources* group in the PSAT is the sum of the contributions from the many small activities that the PMF cannot distinguish individually, as well as the boundary conditions that account for less than 1% of $PM_{2.5}$ on average in the considered period. The global picture obtained when repartitioning the secondary $PM_{2.5}$, quantified by the field campaigns and associated with two main secondary

Table 3
$PM_{2.5}$ source apportionment obtained by CAMx-PSAT in Summer (June–August 2011) and late Autumn (15 November–15 December 2011) in the three monitoring sites. All the concentration values are given in ng m^{-3}.

	Cso Firenze (ng m^{-3})		Multedo (ng m^{-3})		Bolzaneto (ng m^{-3})	
	Summer	Fall–winter	Summer	Fall–winter	Summer	Fall–winter
Road Transport	5600	6900	4100	5400	3600	6300
Maritime	1200	900	800	700	300	500
Residential	100	1500	200	1500	200	1600
Energy Production – Industry	1900	3500	1600	3300	1600	3600
Others	1800	5500	2300	5900	2000	6000

Table 4
$PM_{2.5}$ source apportionment based on PMF and the post-processing discussed in Section 3.5. Values are given in percentage for the period June–August 2011. NR stands for Not Resolved. The $PM_{2.5}$ mass reconstructed by the PMF in the same period in the three monitoring sites is 12577 ng m^{-3}, 12089 ng m^{-3} and 13852 ng m^{-3}, in Corso Firenze, Multedo, Bolzaneto, respectively. Numbers in parentheses are the percentage contributions estimated by CAMx for summer, as deduced by the absolute values given in Table 3. We cannot firmly quantify the major source of uncertainty of the CAMx-PSAT results, i.e. the emission rates in the used inventories. However, we can reasonably assume that PSAT results are affected by uncertainties not smaller than the PMF ones.

	Corso Firenze (%)	Multedo (%)	Bolzaneto (%)
Road Transport	35 ± 10 *(53)*	38 ± 12 *(46)*	38 ± 13 *(47)*
Maritime	15 ± 2 *(11)*	16 ± 3 *(9)*	14 ± 3 *(4)*
Residential	NR *(1)*	NR *(2)*	NR *(2)*
Energy Production – Industry	36 ± 10 *(18)*	27 ± 15 *(18)*	33 ± 12 *(21)*
Others	15 ± 4 *(17)*	18 ± 5 *(25)*	14 ± 4 *(26)*

sources by PMF, was basically confirmed by the CAMx-PSAT analysis, revealing that the emissions related to traffic, energy production and maritime activities contributed approximately 40%–50%, 20%–30% and 15% of the total $PM_{2.5}$ in the summer of 2011, respectively.

4. Conclusions

A source apportionment exercise was performed in Genoa using field data processed by PMF and by exploiting the PSAT tool implemented in the CAMx model. Combining these approaches is not common, and a firm methodology comparing their results is still missing.

We have attempted to overcome the difficulties affecting comparisons between receptor and chemical transport models, particularly for the grouping/classification of PM sources and the apportionment of the secondary components, through a critical analysis of the PMF factor profiles and a limited number of empirical assumptions. Even if the $PM_{2.5}$ apportionment was conservatively considered with quite large uncertainties, it agreed with the CAMx-PSAT estimates. Moreover, the satisfactory performance of the CAMx-PSAT model during the source apportionment exercise revealed that this chemical transport model can be considered a reliable predictive tool.

The methodology presented here is a preliminary approach to the problem; however, it has established that both receptor models for processing field data and chemical transport models based on bottom-up emission inventories might be used synergistically in the future.

Acknowledgements

We thank Mr. Vincenzo Ariola for his technical support. Thanks are due to Regione Liguria (Dr. L. Badalato) and Amministrazione Provinciale di Genova (Dr. M.T. Zannetti) for providing the emission inventory for the city of Genova. We are particularly indebted with Dr. Anastasia Poupkou from the Aristotle University of Thessaloniki for her help in the preparation of CAMx input files.

This work has been supported by European Program MED 2007/2013 through the APICE grant.

Appendix A. Supplementary data

Supplementary data related to this article can be found at http://dx.doi.org/10.1016/j.atmosenv.2014.05.039.

References

Ariola, V., D'Alessandro, A., Lucarelli, F., Marcazzan, G., Mazzei, F., Nava, S., Garcia Orellana, I., Prati, P., Valli, G., Vecchi, R., Zucchiatti, A., 2006. Elemental characterization of PM_{10}, $PM_{2.5}$ and PM_1 in the town of Genoa (Italy). Chemosphere 62, 226–232.

Bates, T., Calhoun, J., Wang, Y., Quinn, P., 1992. Variations in the methanesulphonate to sulphate molar ratio in submicrometer marine aerosol particles over the South Pacific Ocean. J. Geophys. Res. 97, 9859–9865.

Birch, M.E., Cary, R.A., 1996. Elemental carbon-based method for monitoring occupational exposures to particulate diesel exhaust. Aerosol Sci. Technol. 25, 221–241.

Burr, M., Zhang, Y., 2011. Source apportionment of fine particulate matter over the Eastern U.S. Part II: source apportionment simulations using CAMx/PSAT and comparisons with CMAQ source sensitivity simulations. Atmos. Pollut. Res. 2, 299–316.

Cavalli, F., Putaud, J.P., Viana, M., Yttri, K.E., Gemberg, J., 2010. Toward a standardised thermal-optical protocol for measuring atmospheric organic and elemental carbon: the EUSAAR protocol. Atmos. Meas. Tech. 3, 79–89.

Chen, F., Dudhia, J., 2001. Coupling an advanced land-surface/hydrology model with the Penn State/NCAR MM5 modeling system. Part I: model description and implementation. Mon. Weather Rev. 129, 569–585.

Chou, M.-D., Suarez, M.J., 1994. An efficient thermal infrared radiation parameterization for use in general circulation models. NASA Tech. Memo. 104606, 3.

Chow, J.C., Watson, J.G., Pritchett, L.C., Pierson, W.R., Frazier, C.A., Purcell, R.G., 1993. The DRI thermal/optical reflectance carbon analysis system: description, evaluation, and applications in U.S. air quality studies. Atmos. Environ. 27A, 1185–1201.

Chow, J.C., Watson, J.G., 1999. Ion chromatography in elemental analysis of airborne particles. In: Landsberger, S., Creatchman, M. (Eds.), Elemental Analysis of Airborne Particles, vol. 1. Gordon and Breach Science, Amsterdam, pp. 97–137.

Contini, D., Belosi, F., Gambaro, A., Cesari, D., Stortini, A., Bove, M.C., 2012. Comparison of PM_{10} concentrations and metal content in three different sites of the Venice Lagoon: an analysis of possible aerosol sources. J. Environ. Sci. 24 (11), 1954–1965.

Cuccia, E., Bernardoni, V., Massabò, D., Prati, P., Valli, G., Vecchi, R., 2010. An alternative way to determine the size distribution of airborne particulate matter. Atmos. Environ. 44, 3304–3313.

Cuccia, E., Massabò, D., Ariola, Bove, M.C., Fermo, P., Piazzalunga, A., Prati, P., 2013. Size resolved comprehensive characterization of airborne particulate matter. Atmos. Environ. 67, 14–26.

EEA, 2009. EMEP/CORINAIR Emission Inventory Guidebook – 2009. European Environment Agency, Copenhagen.

Environmental Modeling Center, 2003. The GFS Atmospheric Model. NCEP Office Note 442, Global Climate and Weather Modeling Branch, EMC, Camp Springs, Maryland.

ENVIRON, 2010. User's Guide, Comprehensive Air Quality Model With Extensions (CAMx). Version 5.30. ENVIRON International Corporation, Novato, CA.

Escrig, A., Monfort, E., Celades, I., Querol, X., Amato, F., Mingiullon, M.C., Hopke, P.K., 2009. Application of optimally scaled target factor analysis for assessing source contribution of ambient PM_{10}. J. Air Waste Manag. Assoc. 59, 1296–1307.

Favez, O., El Haddad, I., Piot, C., Boreave, A., Abidi, E., Marchand, N., Jaffrezo, J.-L., Besombes, J.-L., Personnaz, M.-B., Sciare, J., Wortham, H., Geroge, C., D'Anna, B., 2010. Inter-comparison of source apportionment models for the estimation of

wood burning aerosols during wintertime in an Alpine city (Grenoble, France). Atmos. Chem. Phys. 10, 5295–5314.
Gordon, G., 1988. Receptor models: development and testing of such models has moved from the research domain into application to practical problems. Environ. Sci. Technol. 22, 1132–1142.
Hertel, O., Berkowics, R., Christensen, J., Hov, O., 1993. Test of two numerical schemes for use in atmospheric transport-chemistry models. Atmos. Environ. 27, 2591–2611.
Huntzicker, J.J., Johnson, R.L., Shah, J.J., Cary, R.A., 1982. Analysis of organic and elemental carbon in ambient aerosols by the thermal-optical method. In: Particulate Carbon: Atmospheric Life Cycle. Plenum Press, New York, pp. 79–88.
Janjic, Z.I., 2002. Non Singular Implementation of the Mellor–Yamada Level 2.5 Scheme in the NCEP Meso model. NCEP Office Note, No. 437.
Kain, J.S., 2004. The Kain–Fritsch convective parameterization: an update. J. Appl. Meteorol. 43, 170–181.
Lee, E., Chan, C.K., Paatero, P., 1999. Application of positive matrix factorization in source apportionment of particulate pollutants in Hong Kong. Atmos. Environ. 33, 3201–3212.
Markakis, K., Katragkou, E., Poupkou, A., Melas, D., 2013. MOSESS: a new emission model for the compilation of model-ready emission inventories—application in a coal mining area in Northern Greece. Environ. Model. Assess. http://dx.doi.org/10.1007/s10666-013-9360-8.
Mason, B., 1966. Principles of Geochemistry. Wiley, New York.
Massabò, D., Bernardoni, V., Bove, M.C., Brunengo, A., Cuccia, E., Piazzalunga, A., Prati, P., Valli, G., Vecchi, R., 2013. A multi-wavelength optical set-up for the characterization of carbonaceous particulate matter. J. Aerosol Sci. 60, 34–46.
Mazzei, F., D'Alessandro, A., Lucarelli, F., Nava, S., Prati, P., Valli, G., Vecchi, R., 2008. Characterization of particulate matter sources in an urban environment. Sci. Total Environ. 401, 81–89.
Miller, M.S., Friedlander, S.K., Hidy, G.M., 1972. A chemical element balance for the Pasadena aerosol. J. Colloid Interface Sci. 39, 65–176.
Mlawer, E.J., Taubman, S.J., Brown, P.D., Iacono, M.J., Clough, S.A., 1997. Radiative transfer for inhomogeneous atmospheres: RRTM, a validated correlated-k model for the longwave. J. Geophys. Res. 102, 16663–16682.
Odman, M.T., Ingram, C.L., 1993. Multiscale Air Quality Simulation Platform (MAQSIP): Source Code Documentation and Validation. Technical report. ENV-96TR002, MCNC–North Carolina Supercomputing Center, Research Triangle Park, North Carolina, p. 83.
Paatero, P., Tapper, U., 1994. Positive matrix factorization: a non-negative factor model with optimal utilization of error estimates of data values. Environmetrics 5, 111–126.
Paatero, P., 1997. Least squares formulation of robust, non-negative factor analysis. Chemom. Intelligent Lab. Syst. 37, 23–35.
Paatero, P., Hopke, P.K., Song, X.H., Ramadan, Z., 2002. Understanding and controlling rotations in factor analytic models. Chemom. Intell. Lab. Syst. 60, 253–264.
Paatero, P., Hopke, P.K., 2003. Discarding or downweighting high-noise variables in factor analytic models. Anal. Chim. Acta 490, 277–289.
Paatero, P., 2010. User's Guide for Positive Matrix Factorization Programs PMF2 and PMF3,22 Part 1: Tutorial. University of Helsinki, Finland.
Pirovano, G., Balzarini, A., Bessagnet, B., Emery, C., Kallos, G., Meleux, F., Mitsakou, C., Nopmongcol, U., Riva, G.M., Yarwood, G., 2012. Investigating impacts of chemistry and transport model formulation on model performance at European scale. Atmos. Environ. 53, 93–109.
Polissar, A.V., Hopke, P.K., Paatero, P., Malm, W.C., Sisler, J.F., 1998. Atmospheric aerosol nucleation and primary emission rates. Atmos. Chem. Phys., 1339–1356.
Poupkou, A., Giannaros, T., Markakis, K., Kioutsioukis, I., Curci, G., Melas, D., Zerefos, C., 2010. Development of a model for the calculation of biogenic NMVOCs emissions in Europe. Environ. Model. Softw. 25 (12), 1845–1856.
Qin, Y., Kim, E., Hopke, P.K., 2006. The concentration and sources of $PM_{2.5}$ in metropolitan New York City. Atmos. Environ. 40, 312–332.
Russell, A., Dennis, R., 2000. NARSTO critical review of photochemical models and modeling. Atmos. Environ. 34, 2283–2324.
Seigneur, C., 2001. Current status of air quality models for particulate matter. J. Air Waste Manag. Assoc. 51 (11), 1508–1521.
Seinfeld, J.H., Pandis, S.N., 1986. Atmospheric Chemistry and Physics. John Wiley & Sons, New York.
Skamarock, W.C., Klemp, J.B., Dudhia, J., Gill, D.O., Barker, D.M., Huang, X.Z., Wang, W., Powers, J.G., 2008. A Description of the Advanced Research WRF Version 3. Technical report. Mesoscale and Microscale Meteorology Division, NCAR, Boulder, Colorado.
Thompson, G., Field, P.R., Rasmussen, R.M., Hall, W.D., 2008. Explicit forecasts of winter precipitation using an improved bulk microphysics scheme. Part II: implementation of a new snow parameterization. Mon. Weather Rev. 136, 5095–5115.
Thurston, G.D., Spengler, J.D., 1985. A quantitative assessment of source contributions to inhalable particulate matter pollution in metropolitan Boston. Atmos. Environ. 19, 9–25.
Viana, M., Kuhlbusch, T.A.J., Querol, X., Alastuey, A., Harrison, R.M., Hopke, P.K., Winiwarter, W., Vallius, M., Szidat, S., Prévôt, A.S.H., Hueglin, C., Bloemen, H., Wåhlin, P., Vecchi, R., Miranda, A.I., Kasper-Giebl, A., Maenhaut, W., Hitzenberger, R., 2008. Source apportionment of particulate matter in Europe: a review of methods and results. J. Aerosol Sci. 39 (10), 827–849.
Wagstrom, K.M., Pandis, S.N., Yarwood, G., Wilson, G.M., Morris, R.E., 2008. Development and application of a computationally efficient particulate matter apportionment algorithm in a three-dimensional chemical transport model. Atmos. Environ. 42, 5650–5659.
Yarwood, G., Rao, S., Yocke, M., Whitten, G., 2005. Updates to the Carbon Bond Chemical Mechanism: CB05. Technical report RT-0400675. US EPA, Res. Tri. Park.
Zhang, Y., Vijayaraghavan, K., Seigneur, C., 2005. Evaluation of three probing techniques in a three-dimensional air quality model. J. Geophys. Res. 110, D02305 http://dx.doi.org/10.1029/2004JD005248.